

# Complex Salts *trans*-[Rh(β-Pic)<sub>4</sub>Cl<sub>2</sub>]X (X = Cl<sup>−</sup>, ReO<sub>4</sub><sup>−</sup>, and ClO<sub>4</sub><sup>−</sup>): Synthesis, Crystal Structures, and Thermal Properties

D. B. Vasil'chenko<sup>a</sup>, \* E. Yu. Filatov<sup>a, b</sup>, I. A. Baidina<sup>a</sup>, P. E. Plyusnin<sup>a, b</sup>, and S. V. Korenev<sup>a, b</sup>

<sup>a</sup> Nikolaev Institute of Inorganic Chemistry, Siberian Division, Russian Academy of Sciences,  
pr. akademika Lavrent'eva 3, Novosibirsk, 630090 Russia

<sup>b</sup> Novosibirsk State University, Novosibirsk, Russia

\*E-mail: scrubber@mail.ru

Received September 24, 2009

**Abstract**—Three novel complex salts containing the cation *trans*-[Rh(β-Pic)<sub>4</sub>Cl<sub>2</sub>]<sup>+</sup> with the anions Cl<sup>−</sup> (**I**), ReO<sub>4</sub><sup>−</sup> (**II**), and ClO<sub>4</sub><sup>−</sup> (**III**) were obtained and characterized by elemental analysis, X-ray diffraction, NMR spectroscopy, and IR spectroscopy. The complex *trans*-[Rh(β-Pic)<sub>4</sub>Cl<sub>2</sub>]ReO<sub>4</sub> crystallizes from DMF as a solvate in which solvent molecules fill the channels formed by the cations and anions. The thermal properties of complexes **I**, **II**, and **II** · DMF were examined by DTA. Final and some intermediate products of the thermolysis were isolated and characterized by physicochemical methods.

**DOI:** 10.1134/S1070328410050052

Rhodium complexes with heterocyclic ligands are thoroughly studied [1] and their catalytic properties are well known [2, 3]. In addition, the antibacterial and anticancer activities of some rhodium(III) complexes with pyridine and its derivatives with aliphatic substituents were widely discussed at different times [4, 5]. Complex salts with the general formula *trans*-[RhA<sub>4</sub>X<sub>2</sub>]Y (where A stands for a heterocyclic ligand) were obtained and characterized by spectroscopic methods over 100 years ago [6]; however, their structural parameters and thermal properties have not been studied in detail hitherto.

Thermolysis of platinum metal complexes containing heterocyclic ligands provides a tool for the synthesis of hybrid organic and inorganic materials with interesting optical properties [7]. Moreover, decomposition of binary complexes of the general formula [M<sup>1</sup>L<sub>n</sub>][M<sup>2</sup>L<sub>m</sub>], (M<sup>1</sup> and M<sup>2</sup> are dissimilar metals, one of which is a noble metal) affords bimetallic powders with different phase compositions [8, 9], which can be widely used in catalytic systems, materials for microelectronics, and magnetic instruments [10]. The preparation of such materials is impossible without detailed and systematic investigations of processes occurring in the thermolysis of the aforementioned compounds. The complex rhodium(III) salts *trans*-[RhA<sub>4</sub>X<sub>2</sub>]Y (where A is pyridine or picolines) are optimal models for such investigations [11] because they contain no complex organic ligands, are relatively easy to obtain in high yields, are stable in storage under normal conditions, and resistant to strong oxidants and strong acids.

Earlier, we synthesized and studied the salts *trans*-[RhA<sub>4</sub>Cl<sub>2</sub>]X (A = Py and γ-Pic (γ-picoline); X<sup>−</sup> = Cl<sup>−</sup>, ClO<sub>4</sub><sup>−</sup>, and ReO<sub>4</sub><sup>−</sup>) [12, 13]. In both ligands A, the substituents and hydrogen atoms in the ring are arranged symmetrically. From this viewpoint, it was interesting to study the structures of similar complexes with β-picoline (an asymmetric ligand) and compare the thermal properties of these complexes.

In this study, we obtained the salts *trans*-[Rh(β-Pic)<sub>4</sub>Cl<sub>2</sub>]Cl · 2H<sub>2</sub>O (**I**), *trans*-[Rh(β-Pic)<sub>4</sub>Cl<sub>2</sub>]ReO<sub>4</sub> (**II**), *trans*-[Rh(β-Pic)<sub>4</sub>Cl<sub>2</sub>]ReO<sub>4</sub> · DMF (**II** · DMF), and *trans*-[Rh(β-Pic)<sub>4</sub>Cl<sub>2</sub>]ClO<sub>4</sub> (**III**) and examined their crystal structures and thermal properties.

## EXPERIMENTAL

**Synthesis of complex I.** A small amount of hydrazine hydrochloride (~6 × 10<sup>−2</sup> mmol) was added to a solution of RhCl<sub>3</sub> (*c*<sub>Rh</sub> = 0.08 mol/l; 5 ml) in 0.5 M HCl. The mixture was heated on a boiling water bath. β-Picoline (1 ml) was added to the vigorously stirred hot solution; the solution turned lemon yellow. The reaction mixture was cooled and mixed with an equal volume of concentrated HCl. The resulting yellow crystals were filtered off, washed with a minimum amount of ice water, and dried in air. The yield was 85%.

For C<sub>24</sub>H<sub>32</sub>Cl<sub>3</sub>N<sub>4</sub>O<sub>2</sub>Rh

anal. calcd. (%): C, 46.65; H, 5.23; N, 9.09; Rh, 16.65.

Found (%): C, 46.55; H, 5.40; N, 9.20; Rh, 17.20.

IR ( $\nu$ ,  $\text{cm}^{-1}$ ): 3393 ( $\nu(\text{O}-\text{H})$ ), 3032 ( $\nu(\text{C}-\text{H})$ ), 1620 ( $\delta(\text{H}_2\text{O})$ ), 1607, 1580 ( $\nu(\text{C}=\text{N})$ ), 1480, 1456, 1414 ( $\nu(\text{C}=\text{C}) + \delta(\text{CH}_3)$ ), 1249, 1185, 1114, 1072, 1040, 804, 701, 663 ( $\delta(\text{CH})$ ), 505, 429, 387 ( $\delta(\text{ring})$ ), 341 ( $\nu(\text{Rh}-\text{Cl})$ ), 236 ( $\nu(\text{Rh}-\text{N})$ ).

$^1\text{H}$  NMR ( $\delta$ , ppm): 8.188 (d, H(5),  $J = 6.2$  Hz), 8.175 (s, H(1)), 7.922 (d, H(3),  $J = 8$  Hz), 7.338 (dd, H(4),  $J_1 = 8$  Hz,  $J_2 = 6.2$  Hz), 2.227 (s, Me).

For  $\beta$ -picoline as a reference compound,  $^1\text{H}$  NMR ( $\delta$ , ppm): 8.809 (d, H(5),  $J = 5$  Hz), 8.707 (s, H(1)), 7.927 (d, H(3),  $J = 7.8$  Hz), 7.688 (dd, H(4),  $J_1 = 7.8$  Hz,  $J_2 = 5$  Hz).

**Synthesis of complex II.** An excess of a saturated solution of sodium perrhenate was added to a hot  $\sim 0.05$  M solution of complex I. The resulting light yellow precipitate was filtered off, washed with a minimum amount of water, and dried in air. The yield was 95–98%.

For  $\text{C}_{24}\text{H}_{32}\text{Cl}_2\text{N}_4\text{O}_4\text{ReRh}$

anal. calcd. (%): C, 36.19; H, 3.54; N, 7.03; Rh + Re, 36.31.

Found (%): C, 36.00; H, 3.20; N, 6.40; Rh + Re, 36.30.

IR ( $\nu$ ,  $\text{cm}^{-1}$ ): 3104, 3044, 2923 ( $\nu(\text{C}-\text{H})$ ), 1607, 1581 ( $\nu(\text{C}=\text{N})$ ), 1481, 1456, 1419 ( $\nu(\text{C}=\text{C}) + \delta(\text{CH}_3)$ ), 1245, 1191, 1115, 1070, 1039, 799, 698, 662 ( $\delta(\text{CH})$ ), 905 ( $\nu(\text{Rh}-\text{O})$ ), 503, 430, 390 ( $\delta(\text{ring})$ ), 341 ( $\nu(\text{Rh}-\text{Cl})$ ), 323 ( $\delta(\text{ReO}_4^-)$ ), 236 ( $\nu(\text{Rh}-\text{N})$ ).

**Synthesis of complex III.** An excess of concentrated  $\text{HClO}_4$  was added to a hot  $\sim 0.05$  M solution of complex I. The resulting light yellow precipitate was filtered off, washed with a minimum amount of water, and dried in air. The yield was 95–98%.

For  $\text{C}_{24}\text{H}_{32}\text{Cl}_3\text{N}_4\text{O}_2\text{Rh}$

anal. calcd. (%): C, 32.48; H, 3.33; N, 6.31.

Found (%): C, 32.50; H, 3.20; N, 6.30.

IR ( $\nu$ ,  $\text{cm}^{-1}$ ): 3108, 3031, 2923 ( $\nu(\text{C}-\text{H})$ ), 1610, 1583 ( $\nu(\text{C}=\text{N})$ ), 1481, 1453, 1420 ( $\nu(\text{C}=\text{C}) + \delta(\text{CH}_3)$ ), 1246, 1193, 797, 697, 662 ( $\delta(\text{CH})$ ), 1093 ( $\nu(\text{Cl}-\text{O})$ ), 621 ( $\delta(\text{ClO}_4^-)$ ), 502, 430, 386 ( $\delta(\text{ring})$ ), 340 ( $\nu(\text{Rh}-\text{Cl})$ ), 233 ( $\nu(\text{Rh}-\text{N})$ ). The band  $\delta(\text{CH})$  is partly masked by the broad absorption band  $\nu(\text{Cl}-\text{O})$ .

Salt I is well soluble in water (27.9 g/l). Salts II and III are poorly soluble even in boiling water (0.27 and 0.19 g/l, respectively). All the salts are well soluble in DMF, pyridine, ethanol, and acetone; they are insoluble in hexane.

IR spectra were recorded on a Scimitar FTS 2000 instrument in the 4000–400  $\text{cm}^{-1}$  range (KBr pellets) and a Vertex 80 spectrometer in the 400–100  $\text{cm}^{-1}$  range (polyethylene pellets).  $^1\text{H}$  NMR spectra were recorded on a Bruker DPX-250 spectrometer in  $\text{D}_2\text{O}$  at room temperature with DMSO as a standard. Analyses for C, H, and N were carried out on a Euro EA 3000 instrument. An analysis for the metal content was

performed by calcining weighed samples of the complexes in a quartz tubular vessel in a flow of hydrogen. The vessel was heated to 600°C with a split furnace. Because salt III decomposes explosively at  $\sim 250^\circ\text{C}$ , an analysis for its rhodium content was not made. Thermal analysis of the complexes was carried out on a TG 209 F1 Iris Thermo Microbalance instrument (NETZSCH) under helium in an  $\text{Al}_2\text{O}_3$  crucible (heating rate 10 K/min).

Single crystals of complexes II and III were grown from their saturated solutions in DMF. Air evaporation for seven days gave large yellow crystals suitable for X-ray diffraction analysis. Complex I crystallized from both water and DMF as thin plates unsuitable for X-ray diffraction analysis.

**X-ray diffraction of complexes II · DMF and III.** An array of reflection intensities was collected on a Bruker-Nonius X8Apex automated four-circle diffractometer (a CCD area detector,  $\text{MoK}_\alpha$  radiation, graphite monochromator) at room temperature. Crystallographic parameters and the data collection statistics for complexes II · DMF and III are given in Table 1. The structures were solved by direct methods and refined in the anisotropic and isotropic (for H) approximations. Part of the H atoms was located from difference electron-density maps and part of them was located geometrically. All calculations were performed with the SHELX-97 program package [14]. Theoretical diffraction patterns for these complexes were calculated from single-crystal X-ray diffraction data. Selected bond lengths in complexes III and II · DMF are listed in Table 2. Additional crystallographic parameters have been deposited with the Cambridge Crystallographic Data Collection (nos. 680021 (III) and 680022 (II · DMF); <http://www.ccdc.cam.ac.uk/>).

**X-ray powder diffraction analysis** of polycrystalline samples was carried out on a DRON-RM4 diffractometer ( $\text{CuK}_\alpha$  radiation, reflected-beam graphite monochromator, scintillation detector with amplitude discrimination). To prepare samples, the complexes were suspended in hexane and applied to the polished side of a fused quartz cell. A similarly prepared sample of polycrystalline silicon ( $a = 5.4309$  Å) was used as an external standard. Diffraction patterns were recorded in the step mode:  $2\theta = 5^\circ$ – $60^\circ$  for the complex salts and  $2\theta = 5^\circ$ – $135^\circ$  for their thermolysis products. The complexes contain the only phase, which is evident from single-crystal X-ray diffraction data.

X-ray powder diffraction analysis of thermolysis products was carried out with consideration to the data contained in the PDF card file for pure compounds [15]. The parameters of the metallic phases were refined for the whole array of data with the PowderCell 2.3 application [16].

**Table 1.** Crystallographic parameters and the data collection and refinement statistics for salt **III** and solvate **II** · DMF

Parameter	Value	
	<b>II</b> · DMF	<b>III</b>
FW	869.61	645.76
Space group	<i>P</i> 1̄	<i>P</i> 4/n
<i>a</i> , Å	10.7300(4)	11.35310(10)
<i>b</i> , Å	11.7134(4)	11.35310(10)
<i>c</i> , Å	14.4452(4)	10.3220(2)
$\alpha$ , deg	69.9970(10)	90
$\beta$ , deg	69.0310(10)	90
$\gamma$ , deg	73.9450(10)	90
<i>V</i> , Å <sup>3</sup>	1568.26(9)	1330.43(3)
$\rho_{\text{calcd}}$ , g/cm <sup>3</sup>	1.842	1.612
<i>Z</i>	2	2
$\theta$ scan range, deg	2.10–32.60	1.97–30.52
Number of measured/independent reflections	14 786/12 573	2040/1883
Ranges of <i>h</i> , <i>k</i> , and <i>l</i> indices	$-16 < h < 15$ $-17 < k < 17$ $-12 < l < 21$	$-10 < h < 16$ $-16 < k < 12$ $-14 < l < 14$
GOOF on <i>F</i> <sup>2</sup>	1.031	1.062
$\Delta\rho_{\text{max}}, \Delta\rho_{\text{min}}$ , e Å <sup>-3</sup>	1.434, -0.982	0.470, -0.313
Number of parameters refined	529	112
<i>R</i> <sub>1</sub> and <i>wR</i> <sub>2</sub> , <i>I</i> > 2σ( <i>I</i> )	<i>R</i> <sub>1</sub> = 0.0292, <i>wR</i> <sub>2</sub> = 0.0608	<i>R</i> <sub>1</sub> = 0.0181, <i>wR</i> <sub>2</sub> = 0.0485
<i>R</i> <sub>1</sub> and <i>wR</i> <sub>2</sub> for all reflections	0.0383, 0.0635	0.0211, 0.0498

## RESULTS AND DISCUSSION

As in the case of pyridine and  $\gamma$ -picoline, a substitution reaction of a solution of RhCl<sub>3</sub> in HCl with  $\beta$ -picoline catalyzed by reducing agents affords the cation *trans*-[Rh( $\beta$ -Pic)<sub>4</sub>Cl<sub>2</sub>]<sup>+</sup>. The hydrate *trans*-[Rh( $\beta$ -Pic)<sub>4</sub>Cl<sub>2</sub>]Cl · 2H<sub>2</sub>O crystallizes in concentrated HCl. Because of its fairly high solubility, ~15–20% of rhodium remains in solution. Salts **II** and **III** are poorly soluble in water and can be isolated from an aqueous solution of complex **I** in nearly quantitative yields.

Recrystallization of salt **II** from DMF results in the formation of solvate **II** · DMF, which is not the case of salt **III** (X-ray diffraction data). The crystal structures contain the octahedral cation *trans*-[Rh( $\beta$ -Pic)<sub>4</sub>Cl<sub>2</sub>]<sup>+</sup> (Fig. 1), the tetrahedral anions ReO<sub>4</sub><sup>-</sup> and ClO<sub>4</sub><sup>-</sup>, and DMF molecules (in solvate **II** · DMF). In the octahedral cation, the NRhN angles vary from 89.00(32)° to 91.60(36)° and the CIRhN angles vary from 88.80(24)° to 91.70(31)°. The dihedral angles between the planes of four Py rings and the equatorial plane RhN<sub>4</sub> (40.5(3)°–49.3(4)°) shape the cation into “a

propeller with four blades”. Such a propeller can be dextro- and levorotatory. In addition, because of the asymmetric structure of Pic ligands, the methyl group can be oriented upward or downward relative to the plane for a particular direction of the propeller’s rotation. However, the salts obtained contain both the “right” and “left” cation forms and the methyl groups of Pic ligands are aligned in all the cations. The bond lengths and bond angles in the tetrahedral anions do not deviate much from the standard values and agree with our previous data [12, 13].

It should be noted that crystals of both complexes were grown from DMF, but only perrhenate salt **II** forms a solvate with DMF. This can be explained by the nonequivalence of the geometrical parameters of the anions. In the crystal structure of perchlorate **III**, the packing of four cations makes a cavity for the anion. The ClO<sub>4</sub><sup>-</sup> anion fits exactly into the cavity. However, the larger ReO<sub>4</sub><sup>-</sup> anion (Re—O, 1.7 Å; Cl—O, 1.44 Å) cannot accommodate itself to this cavity, forming a more strained structure. When salt **II** crys-

**Table 2.** Selected bond lengths in structures **II** · DMF and **III**\*

Bond	<i>d</i> , Å	Bond	<i>d</i> , Å
<b>II</b> · DMF			
Re(1)–O(1)	1.720(8)	C(12)–C(13)	1.363(14)
Re(1)–O(2)	1.722(7)	C(13)–C(14)	1.399(14)
Re(1)–O(4)	1.725(8)	C(14)–C(15)	1.412(11)
Re(1)–O(3)	1.728(8)	C(14)–C(16)	1.500(13)
Rh(1)–N(4)	2.047(8)	C(21)–C(22)	1.352(14)
Rh(1)–N(3)	2.054(8)	C(22)–C(23)	1.410(14)
Rh(1)–N(2)	2.056(8)	C(23)–C(24)	1.386(13)
Rh(1)–N(1)	2.057(9)	C(24)–C(25)	1.419(13)
Rh(1)–Cl(2)	2.340(3)	C(24)–C(26)	1.470(12)
Rh(1)–Cl(1)	2.347(3)	O(1A)–C(1A)	1.218(13)
N(1)–C(15)	1.342(13)	C(1A)–N(1A)	1.337(14)
N(2)–C(25)	1.352(12)	N(1A)–C(3A)	1.422(13)
C(11)–C(12)	1.410(12)	N(1A)–C(2A)	1.475(14)
<b>III</b>			
Rh(1)–N(1)	2.066(1)	Cl(3)–O(1) <sup>vi</sup>	1.4418(10)
Rh(1)–N(1) <sup>i</sup>	2.066(1)	N(1)–C(5)	1.3495(15)
Rh(1)–N(1) <sup>ii</sup>	2.066(1)	N(1)–C(1)	1.3512(15)
Rh(1)–N(1) <sup>iii</sup>	2.066(1)	C(1)–C(2)	1.3890(16)
Rh(1)–Cl(2)	2.3414(6)	C(2)–C(3)	1.3858(18)
Rh(1)–Cl(1)	2.3542(6)	C(2)–C(6)	1.4987(19)
Cl(3)–O(1)	1.4418(10)	C(3)–C(4)	1.3789(19)
Cl(3)–O(1) <sup>iv</sup>	1.4418(10)	C(4)–C(5)	1.3849(18)
Cl(3)–O(1) <sup>v</sup>	1.4418(10)		

\* The symmetry operation codes for equivalent atoms of **III** are: <sup>i</sup> 1.5 – *x*, 1.5 – *y*, *z*; <sup>ii</sup> 1.5 – *x*, *y*, *z*; <sup>iii</sup> *x*, 1.5 – *y*, *z*; <sup>iv</sup> 1.5 – *x*, 0.5 – *y*, *z*; <sup>v</sup> –0.5 + *x*, 1 – *y*, 1 – *z*; <sup>vi</sup> 1 – *x*, 0.5 + *y*, 1 – *z*.

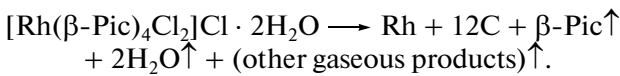
tallizes from DMF, the formation of solvate **II** · DMF becomes more favorable. Similar structural features were observed for the salt  $[\text{RhPy}_4\text{Cl}_2]\text{ReO}_4$ , which crystallizes as both this salt and its dehydrate.

The general view of structure **II** · DMF is shown in Fig. 2. Dimethylformamide molecules are in the channels formed by the cations and anions. The dipole moments of adjacent DMF molecules are collinear but oppositely directed. Thus, the dipolar interactions additionally stabilize the solvate structure. The Cl–Rh–Cl axes of the cations are all perpendicular to the plane (0011). The shortest distances are Rh···Rh (6.841 Å) and Rh···Re (6.782 Å).

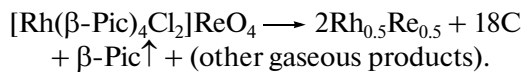
The crystal structure **III** (Fig. 3) can be represented as a system of cation-formed channels aligned with the axis *z*. In this structure, the Cl–Rh–Cl axes are par-

allel to the axis *z* and the cations are stacked. The shortest Cl···Cl distance between the cations in the stack is 5.627 Å. Each of the aforesaid channels is made up of four such stacked structures. The anions are inside the channels. A similar structure was found in the clathrate *trans*-[MnPy<sub>4</sub>(CNS)<sub>2</sub>] · Py [17], in which neutral *trans*-[MnPy<sub>4</sub>(CNS)<sub>2</sub>] molecules form channels for pyridine molecules.

The thermal stability of the salts obtained depends on the anion nature. For instance, salt **I** (Fig. 4a) begins to decompose at ~100°C, releasing two water molecules into the gaseous phase. In the next step, one β-picoline molecule is replaced by a chloride ion to give a mixture of isomers  $\text{Rh}(\beta\text{-Pic})_3\text{Cl}_3$ . In a separate experiment, the released substance was condensed and identified as β-picoline (<sup>1</sup>H NMR data). In the TG curve, this step is virtually immediately followed by the third one. In this step, as with the salt  $[\text{Rh}(\gamma\text{-Pic})_4\text{Cl}_2]\text{Cl} \cdot 2.5\text{H}_2\text{O}$ , first another β-picoline molecule is removed to form a polymeric product and then the organic ligand undergoes thermal degradation. The final thermolysis products are metallic rhodium and amorphous carbon. The weight of the thermolysis products agrees with the following scheme:



The decomposition of salt **II** (Fig. 4b) begins at ~300°C and is accompanied by the weight loss corresponding to the removal of a β-PicHCl molecule. The hydrogen atom required to form HCl can be released as a result of C–Rh or C–C (between two β-picoline molecules) bond formation. This step produces a black resinous substance that solidifies into a glassy mass upon cooling. The substance is insoluble in water or organic solvents; its IR spectrum retains characteristic absorption bands of the perrhenate anion. With an increase in the temperature, the organic ligand degrades and the final thermolysis product is a mixture of amorphous carbon and the solid solution  $\text{Rh}_{0.5}\text{Re}_{0.5}$ . The experimental weight of the final thermolysis product corresponds to the overall scheme:



Solvate **II** · DMF releases a DMF molecule at ~110°C (Fig. 4c). According to X-ray powder diffraction data, the first-step product is structurally identical with the starting pure salt **II**. At higher temperatures, the TG curve is shaped like that of salt **II** described above and has the same quantitative characteristics.

The perchlorate salt decomposes explosively at >270°C; so its thermal transformations were not studied.

Thus, for the salts containing the cation *trans*-[ $\text{Rh}(\beta\text{-Pic})_4\text{Cl}_2$ ]<sup>+</sup> with the anions  $\text{Cl}^-$ ,  $\text{ClO}_4^-$ , and  $\text{ReO}_4^-$ , the dependence of the thermal properties on

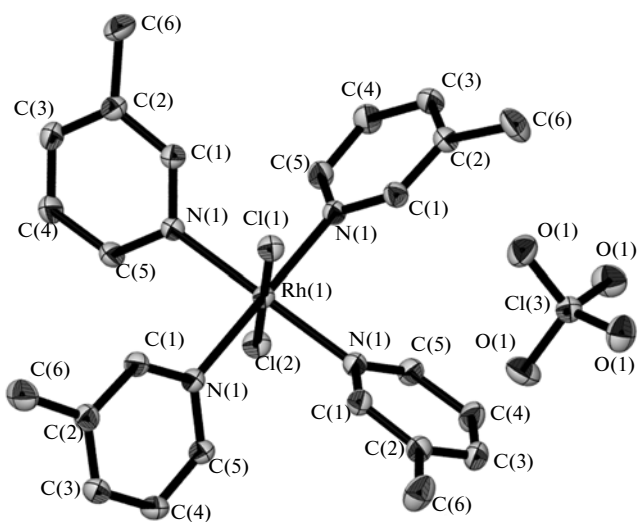


**Fig. 1.** Structure **III** (hydrogen atoms are omitted).

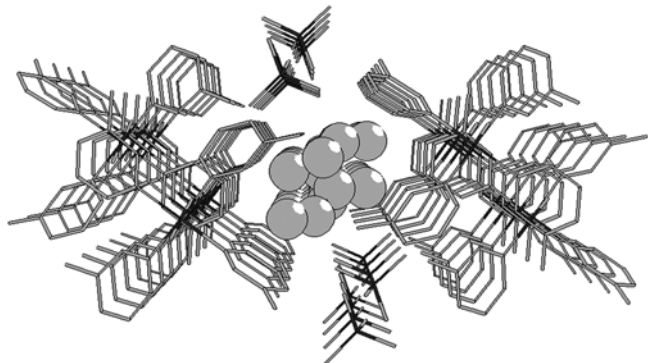


**Fig. 2.** General view of the structure of solvate **II** · DMF along the axis *y*. DMF molecules are shown as balls with the respective van der Waals radii.

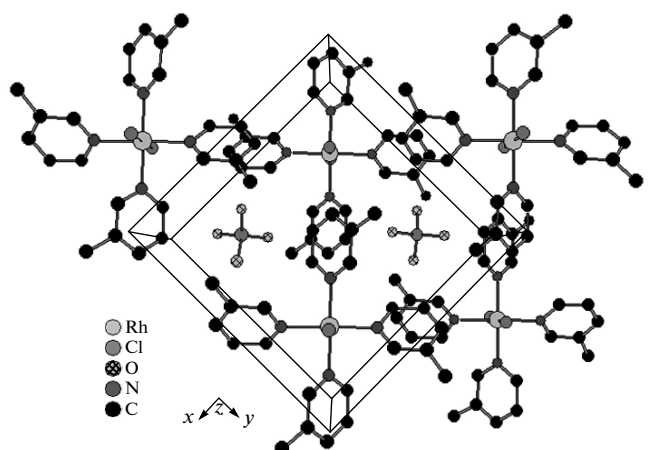


**Fig. 3.** General view of the crystal structure of salt **III**.

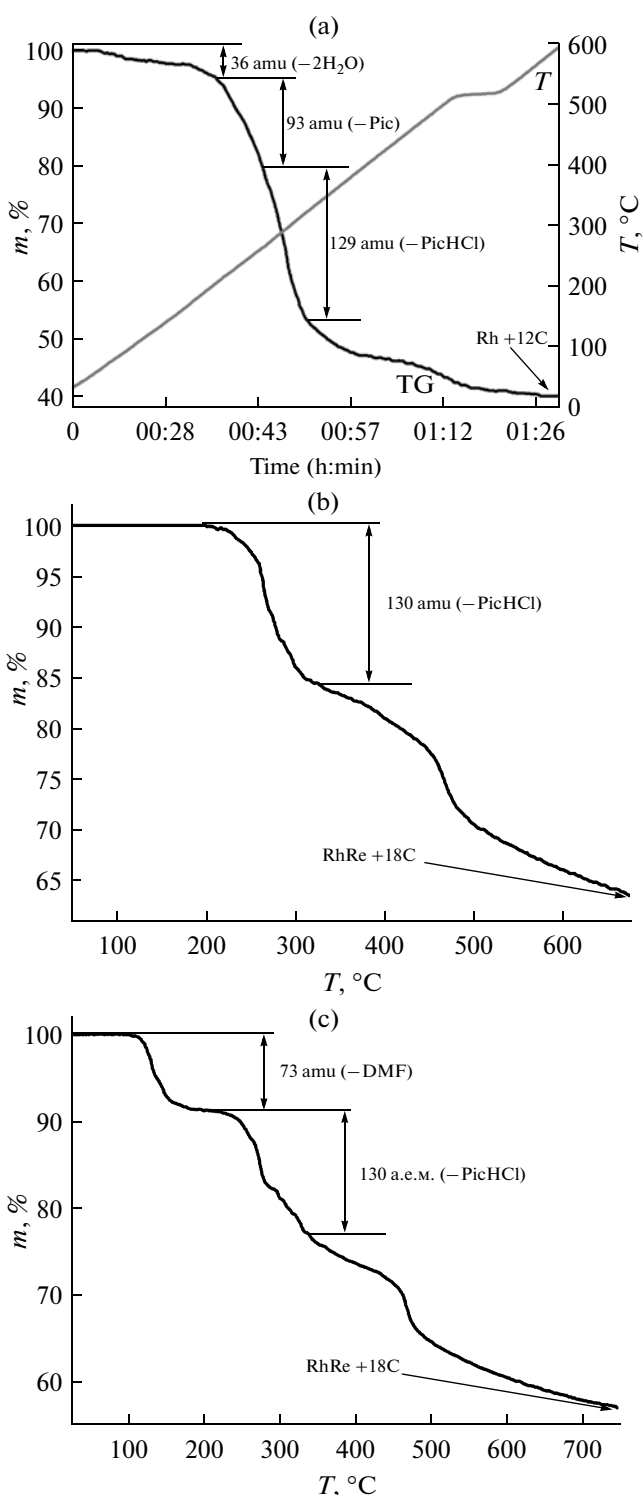


**Fig. 4.** TG curves of (a) salt **I**, (b) salt **II**, and (c) solvate **II** · DMF.

the composition is of the same fundamental character as for related complexes with pyridine and  $\gamma$ -picoline. However, the steps in the thermolysis of salt **I** are not well resolved, which is probably due to the closer temperatures at which the corresponding processes start.

Note that the cations *trans*-[Rh( $\beta$ -Pic)<sub>4</sub>Cl<sub>2</sub>]<sup>+</sup> and [RhPy<sub>4</sub>Cl<sub>2</sub>]<sup>+</sup> have close sizes and form similar structures (e.g., solvation of perrhenate salts). The salt [Rh( $\gamma$ -Pic)<sub>4</sub>Cl<sub>2</sub>]ReO<sub>4</sub> forms no solvates because the cavities made by the cation packing are noticeably larger and can accommodate both perchlorate and perrhenate ions.

### ACKNOWLEDGMENTS

We are grateful to N.V. Kurat'eva for performing X-ray diffraction experiments, N.I. Alferova for her assistance in recording the IR spectra, and I.V. El'tsov for recording the NMR spectra and for his assistance in their interpretation.

### REFERENCES

- Jardine, F.H and Sheridan, P.S, in *Comprehensive Coordination Chemistry*, Gillard, R.D., Wilkinson, G., and McCleverty, J.A., Eds., Oxford: Pergamon, 1987, vol. 2, p. 995.
- Balzani, V., Juris, A., Venturi, M., et al., *Chem. Rev.*, 1996, vol. 96, p. 759.
- Modern Rhodium-Catalyzed Organic Reactions*, Evans P.A., Ed., Weinheim: Wiley-VCH, 2005.
- Gillard, R.D. and Lekkas, E., *Transition Met. Chem.*, 2000, vol. 25 P, p. 617.
- Aceto, M. and Martin, B.R., *J. Med. Chem.*, 1979, vol. 22 P, p. 174.
- Jorgensen, S.M., *J. Prakt. Chemie*, 1885, vol. 27, p. 478.
- Aleksandrova, E.L. and Khimich, N.N., *Fiz. Tekh. Poluprovodn. (St.-Peterburg)*, 2004, vol. 38, no. 11, p. 1280 [*Semiconductors* (Engl. Transl.), vol. 38, no. 11, p. 1280].
- Korenev, S.V., Venediktov, A.B., Shubin, Yu.V., et al., *Zh. Strukt. Khim.*, 2003, vol. 44, no. 1, p. 74.
- Zadesenets, A.V., Filatov, E.Yu., Yusenko, K.V., et al., *Inorg. Chim. Acta*, 2008, vol. 361, p. 199.
- Toshima, N. and Yonezawa, T., *New J. Chem.*, 1998, p. 1179.
- Kovrova, N.B., Bondarenko, V.S., Korniets, E.D., et al., *Zh. Obshch. Khim.*, 1994, vol. 64, p. 885.
- Vasil'chenko, D.B., Baidina, I.A., Filatov, E.Yu., and Korenev, S.V., *Zh. Strukt. Khim.*, 2009, vol. 50, no. 2, p. 349.
- Korenev, S.V., Vasil'chenko, D.B., Baidina, I.A., et al., *Izv. Akad. Nauk, Ser. Khim.*, 2008, no. 8, p. 1607.
- Sheldrick, G.M., *SHELX-97. Release 97-1*, Göttingen (Germany): Univ. of Göttingen, 1997.
- PCPDFWin. Version 1.30. JCPDS ICDD. Swarthmore (PA, USA), 1997.
- Kraus, W. and Nolze, G., *Powder Cell 2.4. Program for the Representation and Manipulation of Crystal Structures and Calculation of the Resulting X-Ray Powder Patterns*, Berlin: Federal Institute for Materials Research Testing, 2000.
- Lipkowski, J. and Soldatov, D.V., *J. Incl. Phenom.*, 1994, vol. 18, p. 317.